Thesis Paper

Effects of Hydrogenphosphate Quenching on Fluorescent Lifetime of Hydroxyphenyl Substituted Diazaoxatriangulenium

Stine Grønfeldt Stenspil*

5

Fluorophores are used in many research applications such as cell staining and as probes for ions, DNA, proteins or membranes. By designing and synthesising the fluorophore to have specific photophysical properties it is possible to probe the surrounding environment of the fluorophore. For example, by utilising the property of photoinduced electron transfer (PET) which quenches the fluorescence of the fluorophore. 10 A hydroxyphenyl substituted diazaoxatriangulenium (DAOTA$^+$) designed to have the properties as a pH probe using photoinduced electron transfer showed another pH dependency in addition to the expected quenching. Results show that hydrogenphosphate is the reason for the additional quenching and other ions is also shown to have quenching abilities. Further understanding of this mechanism could result in a new triangulenium derivative that is able to detect hydrogenphosphate or other ions in solution. The detection 15 of hydrogenphosphate is especially interesting as it is a key component in physiological solutions and cells.

Introduction

Triangulenium dyes are organic fluorophores consisting of carbon rings linked together either with oxygen,[1] nitrogen[2] or carbon[3] bridges forming a triangular planar and rigid structure with a 20 carbocation in the centre. The rigidity of these dyes gives them advantage of long lifetimes of 10-20 ns and large quantum yields compared to other well-known fluorophores.[4] The longer lifetimes give the possibility of high contrast images of cells using time gating. This is possible because the triangulenium fluorescence is 25 still measurable after the auto luminescence of the cell has fallen in intensity.[3] The triangulenium dyes can have many different applications depending on the substitution groups on the nitrogen bridges. Using a biolinker, the fluorophore can bind to proteins and then be used to study protein motion and interactions.[5] If an 30 "antenna" in the form of a dye with high absorption coefficient is used the fluorescence signal of the triangulenium will be enhanced with the help of energy transfer. These types of fluorophores are known as dyads and can be used in cellular imaging with the advantage of high fluorescence intensity and long lifetime.[6]

35 Many fluorescent compounds are synthesized and used as probes in biological and medical research. There are probes designed for the detection of ions such as Ca^{2+}, Mg^{2+}, Na^+, K^+ and as pH sensors.[7] Fluorescein and its charged derivatives are examples of pH responsive fluorescent probes, which are among some of the 40 first fluorescent pH sensors used.[8] However, they undergo rapid photobleaching making them less useful for measurements over longer periods of time. Tuning the triangulenium fluorophore using a phenol Figure 1A as substitution group makes the dye an efficient pH probe.[9] This is possible by taking advantage of 45 intramolecular photoinduced electron transfer (PET). In Figure 1C
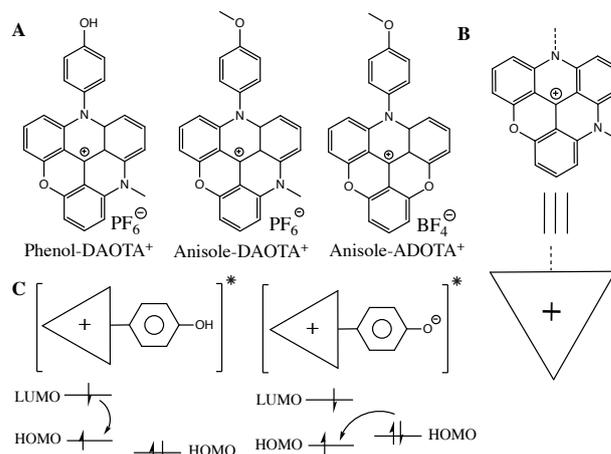
Figure 1: A: Molecular structure of hydroxyaryl diazaoxatriangulenium (Phenol-DAOTA$^+$), methoxyaryl diazaoxatriangulenium (Anisole-DAOTA$^+$) and methoxyaryl azadioxatriangulenium (Anisole-ADOTA$^+$). 50 **B**: Schematic representation of the diazaoxatriangulenium. **C**: Schematic drawing of photoinduced reductive electron transfer. The exited electron in the LUMO for the phenol form is free to deactivate by photon emission. For the phenolate the HOMO of the donor is raised and the HOMO of the fluorophore is occupied due to the larger PET efficiency preventing the 55 exited electron in the LUMO to deactivate.

the mechanism is shown. An electron in the HOMO of the fluorophore is exited to the LUMO. Another electron is transferred from the donor (the phenol) to the fluorophore and thus occupying the HOMO and preventing the exited electron to return to ground 60 state while emitting a photon.[10] In this case when the fluorophore is in acidic solution it is in its phenol form and will fluoresce, while in basic solution the phenolate form will dominate and the dye is

quenched. Using this fluorophore as pH sensor gives the possibility to measure the pH over increased periods of time due to its good photostability.[3, 11]

Previous work has characterized the phenol substituted DAOTA$^+$ in meta, ortho or para positions.[9] During photophysical characterization a small fluorescence quenching was observed before the major PET quenching as a result of pH change. Analysis of the lifetimes also showed a clear pH dependent decrease. The change in fluorescent lifetime showed that it was not related to the phenol/phenolate reaction as only the lifetime of the unquenched fluorophore should be present. Due to this small quenching not being near the phenol/phenolate equivalence point it must be a property of the solvent interacting with the dye and not connected to the pH related deprotonation. As the measurements were made in a phosphate buffered saline (PBS) and dimethylsulfoxide (DMSO) solution it could be hydrogen bonds to the hydroxyl group lowering its HOMO resulting in an extra fluorescence "on" state. There is also the possibility it is the salts in the solution which are shielding or deprotonating the fluorophore through some form of mechanism.

In this paper the compound of interest hydroxyphenyl diazaoxatriangulenium (phenol-DAOTA$^+$) Figure 1A was examined in various solvent compositions. The most similar derivative without possibility of deprotonation is the methoxyphenyl derivative shown in Figure 1A. This donor was examined with two different triangulenium acceptors shown in Figure 1A: diazaoxatriangulenium (anisole-DAOTA$^+$) and azadioxatriangulenium (anisole-ADOTA$^+$). Change of the solution parameters showed that it is hydrogenphosphate deprotonating the exited state of the phenol-DAOTA$^+$ when colliding with it and thus quenching the dye. Other ions were also investigated for their quenching abilities showing both hydroxide and acetate ions having an effect on the phenol-DAOTA$^+$ lifetime however not in the same degree as hydrogenphosphate.

With some improvement this property could be exploited for the detection of hydrogenphosphate in solution. Other dyes have been synthesized for sensing of hydrogenphosphate or other anions by using the chelate effect or an anion receptor linked to the fluorophore among many other approaches.[12-14] The influence of hydrogenphosphate is also important to have in mind if the fluorophore is used in biological research detecting the pH as there is significant phosphate concentration in solution under physiological conditions and in cells.

In the paper by Zelent et al. they have observed the same quenching properties of phosphate on pyrene-1-carboxylate when dihydrogenphosphate protonates the fluorophore.[15] They find a correlation of ΔpK and quenching efficiency between fluorophore and quencher which is as predicted by the Marcus theory. Initial results found during this project show the similar relationship between quenching and ΔpK.

Results and discussion

pH dependency of the phenol-DAOTA$^+$ and anisole-DAOTA$^+$

The phenol-DAOTA$^+$ in PBS and DMSO has previously shown a pH dependency of fluorescence and lifetime decay related to the deprotonation of the hydroxy group. This quenching is due to
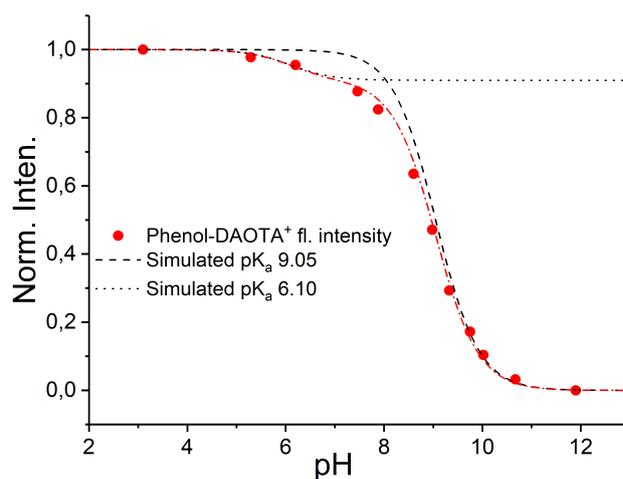
Figure 2: Normalized fluorescence intensity for the phenol-DAOTA$^+$ in PBS (red circles) showing a weak (black dotted) and a strong (black dashed) forms of quenching with pK$_a$ 9.05 and 6.10 respectively. The red line is the combination of the two simulations.

photoinduced reductive electron transfer (PET). But as described another 9% of the total quenching with a pK$_a$ lower than that of the quenching by PET was also observed. In this project these results were repeated with a slightly higher DMSO concentration as precipitation of the fluorophore otherwise was observed in basic pH. This is described further in the supplementary information section S3. The quenching of the fluorophore is shown in Figure 2 where the fluorescence, normalized with respect to the maximum intensity, shows the deprotonation related quenching with pK$_a$ 9.05 and the smaller quenching with an approximate pK$_a$ 6.10. Analysis of the lifetime Figure S8 left showed that the smaller quenching also resulted in a decrease in fluorescent lifetime. The absorbance spectra Figure S5 shows an isosbestic point which means that there is a pure conversion from the phenol to phenolate and no other reaction takes place as a side effect of the altered pH conditions. The normalized absorption intensities figure S6 were used to determine the pK$_a$ of the pH related deprotonation to be 9.05 as the absorption is only influenced by this and not the unknown quenching.

All the lifetime measurements showed monoexponential decays (section S4) indicating that there is only one fluorescent compound in solution. But due to the lifetime decrease being quite small at only 9% it can be challenging to choose the correct model for fitting because the difference will only be visible by single photon counts at times over 30 ns after excitation. These small variances are often hidden in the background noise. Another pitfall to be aware of is the fitting of biexponential decays, as the many variables give the possibility of fitting different amplitudes and lifetimes to the same dataset with little variance.[8, 16] This issue is elaborated further in the SI section S2. Having this in mind, it is not possible to conclude on the quenching mechanism being either dynamic or static using just the initial measurements.

As the pK$_a$'s of the quenching found from the lifetime data and the pH induced deprotonation are not similar it is possible that it is a quenching related to the solvent composition. The quenching of the lifetime cannot be related to the hydroxide concentration as [OH$^-$] keeps increasing with increasing pH. This would result in a continuous decrease of the lifetime but the data show that the
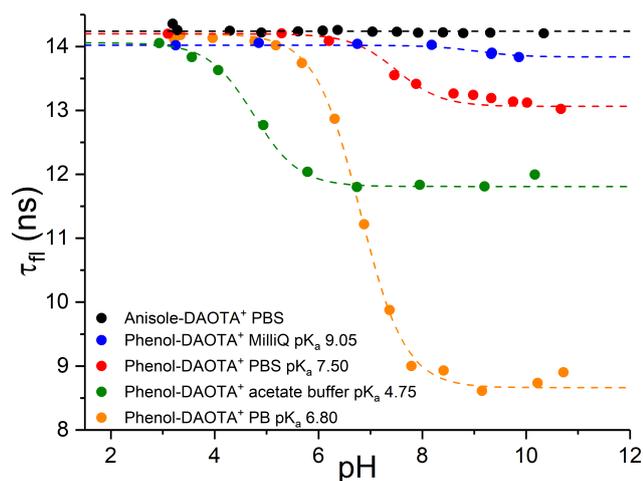
Figure 3: Fluorescent lifetimes of the phenol-DAOTA$^+$ in PB (orange), PBS (red), MilliQ (blue) and acetate buffer (green) showing the pH dependency in the different solutions. The anisole-DAOTA$^+$ (black) is shown as a constant lifetime reference.
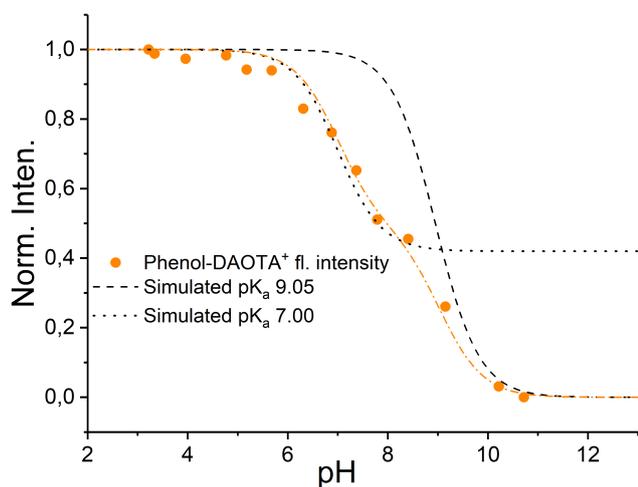
Figure 4: Normalized fluorescence intensity for the phenol-DAOTA$^+$ in PB (orange circles) showing a quenching with pK$_a$ 7.0 (black dotted) and another with pK$_a$ 9.05 (black dashed) forms of quenching. The orange line is the combination of the two simulations.

quenching reaches a saturation point at ~13 ns and does not decrease further. The anisole-DAOTA$^+$ was examined under the same conditions but did not show the quenching found for the phenol-DAOTA$^+$ both for the fluorescence intensity and lifetime as seen in Figure S9 and Figure 3. As there was a possibility of the methoxy group having lowered the donor HOMO orbital interfering with the mechanism, a more electron accepting fluorophore the anisole-ADOTA$^+$ was also examined in acidic and basic solution where the results are shown in Table S1 but no pH dependent lifetime was observed. Increasing the DMSO concentration to 30v% and measuring the fluorescent intensities and lifetimes (Table S1) did not show any effect either. These results rule out the possibility of the small quenching being hydrogen bonding, lowering the donor molecular orbital and thereby the PET efficiency which would result in a more fluorescent state than without hydrogen bonding.

Changing the buffer from PBS to phosphate buffer (PB) showed a significantly larger lifetime decrease at 36% of the longest lifetime
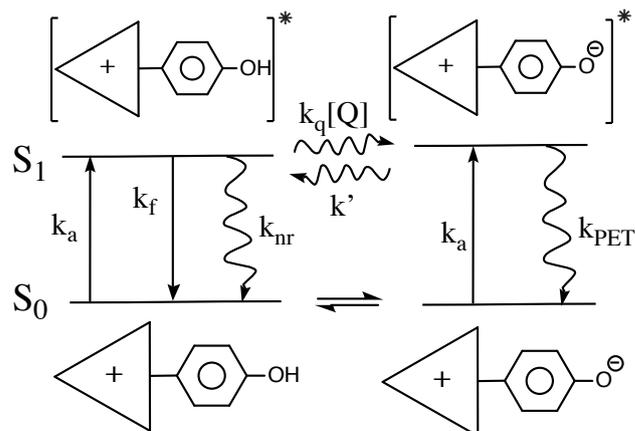
Figure 5: Jablonski diagram for the phenol-DAOTA$^+$ illustrating the ground state S$_0$ and first exited state S$_1$ and the processes affecting fluorescence. The constants k$_f$ and k$_{nr}$ are assumed constant and can be describes as one rate constant for deactivation k$_d$. As k$_{PET}$>>k' the phenolate is not protonated while in exited state which means a deprotonation by the quencher Q results in fluorescence quenching.

(Figure 3). This effect had a similar percentage fluorescence intensity quenching (Figure 4). The difference between the two buffers were a higher phosphate concentration and with no NaCl in solution giving reason to believe that it is an ion related quenching.

Ion related quenching

A control experiment was performed using no buffer but only MilliQ water adjusted to various pH values. Figure 3 shows only a very small decrease in lifetime with pK$_a$ 9.05. This determines that it is phosphate quenching the phenol-DAOTA$^+$ in a collisional process by deprotonating the fluorophore in its exited state resulting in immediate PET. In Figure 5 a Jablonski diagram shows the rate constants related to the excitation and deactivation of the fluorophore all having an influence on the fluorescent lifetime. All deactivation not related to the quencher is assumed constant as the triangulenium remains unchanged. The fluorescent lifetime can therefore be described as $\tau = 1/(k_d + k_q[Q])$, where k$_d$ is the rate of deactivation of the fluorophore k$_d$ = k$_f$ + k$_{nr}$. The pK$_a$ at approximately 6.80 shows that it must be hydrogenphosphate having the major quenching effect and not dihydrogenphosphate. By using the Henderson-Hasselbalch equation to calculate the concentration of HPO$_4^{2-}$ when the pH value in solution is known, it was possible to plot the data and fit it according to the Stern-Volmer equation 1.

$$\frac{\tau_0}{\tau} = 1 + k_q\tau_0[Q] \qquad 1$$

The lifetimes are used, because the fluorescence intensity is also affected by the deprotonation quenching due to pH. The data show a good linear relationship as shown in Figure 6 which confirms that it is a dynamic quenching of the phenol-DAOTA$^+$ by HPO$_4^{2-}$. The total quenching of the phenol-DAOTA$^+$ can therefore be described as a combination of dynamic quenching by collision of ions with the phenol-DAOTA$^+$ in exited state and static quenching by pH dependent deprotonation to the phenolate in ground state.
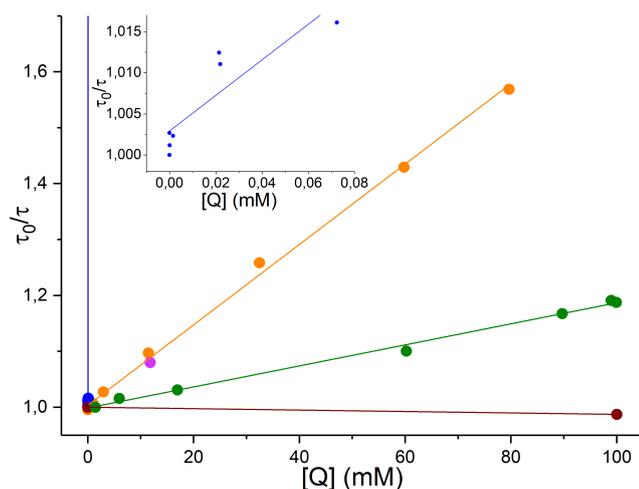
Figure 6: Stern-Volmer plot for the quenching ions. OH⁻ (blue) with a very steep slope has strong quenching abilities. The inset shows the data points for OH⁻ as the concentration is significantly smaller than for the other ions. HPO₄²⁻ (orange) and CH₃COO⁻ (green) also shows quenching properties. Cl⁻ (darkred) show no quenching with no change in lifetime between 0mM and 100mM, the third point from PBS at basic pH 11.8mM HPO₄²⁻ and 100mM Cl⁻ (violet).

Table 1: Properties of the anions in the examined solutions

Anion	k_q[a] ($M^{-1}s^{-1}$)	Diffusion rate[b] (m^2s^{-1})	pKa of conjugate acid[b]	ΔpK[d]
Cl⁻	-	$2.032 \cdot 10^9$	-7/strong acid	-16.05
$H_2PO_4^-$	-	$0.959 \cdot 10^9$	2.16	-6.89
CH_3COO^-	$1.34 \cdot 10^8$	$1.089 \cdot 10^9$	4.756	-4.294
HPO_4^{2-}	$5.10 \cdot 10^8$	$0.759 \cdot 10^9$	7.21	-1.84
OH⁻	$1.54 \cdot 10^{10}$	$5.273 \cdot 10^9$	13.995	4.945

[a] Rate constants calculated from linear regression of the Stern-Volmer plot. [b] Constants found in the Handbook of chemistry and physics 96th edition.[17] [d] Calculated as ΔpK= pKa,acid - pKa,phenol-DAOTA⁺, where pKa,phenol-DAOTA⁺=9.05

Selectivity

PBS, PB, MilliQ water or acetate buffer containing different ions were used as solvents to examine the quenching effects and efficiency of the various ions. The pH dependencies of the phenol-DAOTA⁺ fluorescence lifetime are shown in Figure 3. Using the lifetime data acquired from the pH titrations a Stern-Volmer plot was generated. This is shown in Figure 6 and rate constants for quenching k_q are calculated and shown in Table 1. The initial lifetimes of the phenol-DAOTA⁺ in the PBS (total phosphate concentration 11.8 mM) and PB (total phosphate concentration 100 mM) solutions at acidic pH where $H_2PO_4^-$ is the dominating species, were on the same order at ~14 ns as the lifetime measured in MilliQ water and the constant lifetime for the anisole-DAOTA⁺. This indicates that $H_2PO_4^-$ have little to no quenching effect on the phenol-DAOTA⁺. The large k_q for OH⁻ shows that the quenching by OH⁻ is diffusion controlled and that it is a highly efficient quencher, quenching the fluorophore at every collision. This could be due to the very high diffusion rate of the ion or the ability of transferring the proton through a chain of water molecules as described by the Grotthuss mechanism.[18] The reason the fluorescent lifetime only decreases by 1% is due to the very low concentration of OH⁻ in solution even at higher pH. Cl⁻ is shown by rough estimate to have no influence on the quenching of the

dye. $H_2PO_4^-$ have no influence on the phenol-DAOTA⁺ as determined previously. It is therefore possible using the lifetime from PBS at very acidic pH and comparing to the lifetime in MilliQ water. Correlating the lifetime in PBS at more basic pH where [HPO_4^{2-}] is near the total phosphate concentration to the Stern-Volmer plot of the PB titration at 11.8 mM also supports the claim that Cl⁻ has no shielding influence as the violet point Figure 6 shows no significant deviation from the phosphate titration. But a more thorough investigation is needed to establish certainty. The absence of quenching by Cl⁻ can be due to the ion having a pKa so low that it is too weak a base to be able to deprotonate the exited state phenol-DAOTA⁺. Acetate also shows a 16% quenching of maximum for both fluorescence intensity Figure S16 and lifetime Figure 3. It is however smaller than the quenching by hydrogenphosphate which is also visible with the smaller slope in the Stern-Volmer plot and lower k_q constant. This variance could be due to the CH₃COO⁻ being singly charged and therefore not as attracted to the positively charged dye by electrostatic forces compared to HPO_4^{2-}. It could also be related to ΔpKa Table 1 between the base and dye. The diffusion constants mentioned in Table 1 show no correlation to the observed k_q's. However it is possible, that there is a relationship between the ion quenching efficiency and pKa. The stronger the base, the larger k_q is observed. This is the same observation by Zelent et al.[15] where they found a linear relationship between ΔpK and log(k_q) corresponding to the Marcus theory. Using the k_q's (not taking the diffusion rates into account) and ΔpK's from Table 1 to create a preliminary log(k_q) vs ΔpK plot Figure S16 showed a good linear relationship.

Further work

To understand this mechanism further and to confirm the possible relation to the Marcus theory it would be beneficial to examine the fluorophore under other solution conditions containing other types of anions. This could be other organic or inorganic anions such as citrate, nitrate, sulphate or lactate. Competitional studies between hydrogenphosphate and another base would also be interesting as it could give more information on the mechanism and help determine if it is an actual collisional quenching or if the deprotonation also occurs by protons moving through a chain of bridging molecules. Another way to examine the mechanism and maybe improve the selectivity is adding sidechains next to the hydroxyl group either shielding the group or introducing a negative charge with deprotonating capabilities.

Conclusion

The photophysical properties of hydroxyphenyl DAOTA⁺ were investigated to determine the cause for the extra quenching not related to the pH dependent PET mechanism. Results show that the fluorescence and lifetime quenching of the fluorophore previously observed were due to HPO_4^{2-} deprotonating the fluorophore in exited state in a collisional process. Other ions' quenching properties were investigated in connection with this finding showing that both OH⁻ and CH₃COO⁻ also quenches the dye with respectively higher or lower efficiency and that Cl⁻ has no effect. So far the data do not tell the exact reason for this difference in quenching abilities but an explanation could be the ΔpKa is having an influence which is also consisting to the Marcus theory. However further work is needed to reach a final conclusion.

Experimental section

All chemicals and solvents were used as received from Sigma-Aldrich. The buffer solutions were made following recipes from Cold Harbor Springs protocol or from AAT Bioquest.

The pH was measured on a calibrated Mettler-Toledo SevenEasy pH-meter after addition of DMSO to the pH adjusted buffer as the chemical caused the pH to shift unpredictably.

Absorption measurements were carried out on a Perkin-Elmer Lambda spectrometer in the 300-750 nm range. Fluorescence measurement were carried out on an Agilent Technologies Cary Eclipse Fluorescence Spectrophotometer. Lifetime decay measurements were carried out on a FluoroTime 300 instrument from PicoQuant using a pulsed solid-state laser at 560 nm. The decays were analyzed using the FluoFit software from PicoQuant. Further information can be found in the supplementary information.

Acknowledgement

References

*Address: Nano-Science Center & Department of Chemistry, University of Copenhagen, Universitetsparken 5, Building 2 CS14, 2100 København Ø, Denmark.; E-mail: txd908@alumni.ku.dk

1. J. C. Martin and R. G. Smith, *Journal of the American Chemical Society*, 1964, **86**, 2252-2256.
2. L. B. W. and K. F. C., *Angewandte Chemie International Edition*, 2000, **39**, 3432-3434.
3. M. Rosenberg, K. R. Rostgaard, Z. Liao, A. O. Madsen, K. L. Martinez, T. Vosch and B. W. Laursen, *Chemical Science*, 2018, **9**, 3122-3130.
4. I. Bora, S. A. Bogh, M. Santella, M. Rosenberg, T. J. Sørensen and B. W. Laursen, *European Journal of Organic Chemistry*, 2015, **28**, 6351-6358.
5. T. J. Sorensen, E. Thyrhaug, M. Szabelski, R. Luchowski, I. Gryczynski, Z. Gryczynski and B. W. Laursen, *Methods and Applications in Fluorescence*, 2013, **1**, 1-6.
6. BWLgroup, unpublished work.
7. R. Haugland, *The Molecular Probes Handbook*, Life Technologies, 11th edn., 2010.
8. J. R. Lakowicz, *Principles of fluorescence spectroscopy*, Springer, 3rd edn., 2006.
9. M. Rosenberg, A. K. R. Junker, T. J. Sørensen and B. W. Laursen, unpublished work.
10. B. Wardle, *Principles and applications of photochemistry*, Wiley, 1st edn., 2009.
11. Z. Liao, S. A. Bogh, M. Santella, C. Rein, T. J. Sørensen, B. W. Laursen and T. Vosch, *The Journal of Physical Chemistry A*, 2016, **120**, 3554-3561.
12. M. E. Huston, E. U. Akkaya and A. W. Czarnik, *Journal of the American Chemical Society*, 1989, **111**, 8735-8737.
13. T. Gunnlaugsson, A. P. Davis and M. Glynn, *Chemical Communications*, 2001, **24**, 2556-2557.
14. P. D. Beer and P. A. Gale, *Angewandte Chemie - International Edition*, 2001, **40**, 486-516.
15. B. Zelent, J. M. Vanderkooi, R. G. Coleman, I. Gryczynski and Z. Gryczynski, *Biophysical Journal*, 2006, **91**, 3864-3871.
16. A. Grinvald and I. Z. Steinberg, *Analytical Biochemistry*, 1974, **59**, 583-598.
17. W. Haynes and D. Lide, *CRC Handbook of Chemistry and Physics*, Boca Raton, 92nd edn., 2015-2016.
18. C. J. T. de Grotthuss, *Biochimica et Biophysica Acta (BBA) - Bioenergetics*, 2006, **1757**, 871-875.